

CRYSTALLIZATION FOULING ON HEAT TRANSFER SURFACES – 25 YEARS RESEARCH IN BRAUNSCHWEIG

M.W. Bohnet

Institute of Chemical and Thermal Process Engineering
 Technical University of Braunschweig
 Langer Kamp 7, D – 38106 Braunschweig, Germany
 E-mail: m.bohnet@tu-braunschweig.de

ABSTRACT

Fouling research at the Technical University of Braunschweig during the last 25 years is mainly focused on the formation of crystal layers. A model for the description of the fouling process was developed and contentiously expanded. Besides the process parameters such as fluid velocity, pulsating flow, heat flux, pH etc., the properties of the fouling layer itself was examined. Shear strength and porosity were determined and correlated with the fouling resistance. Another focus was put on the interactions between heat transfer surface and the fouling layer. The build-up of the layer was optically observed with the holographic interferometry. Hence concentration and temperature profiles in the immediate vicinity of the wall could be calculated. Structured and modified surfaces were applied to lengthen the induction period.

INTRODUCTION

Forced by industry fouling research began in the late seventies. At this time nobody at German Universities was working in this field. The reason was simple. Doing research means: working for a PhD-thesis. But fouling was at this time not a scientific topic. Besides experimental investigations we focused therefore on the physical/chemical understanding of the fouling process.

FOULING BY CRYSTALLIZATION

Modeling

The deposition of crystals can be described taking diffusion and reaction into account as shown in Fig. 1.

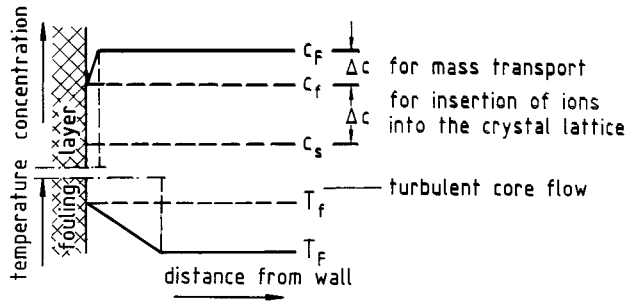


Fig. 1: Concentration and temperature profile in the vicinity of the fouling layer

Mass transfer by diffusion:

$$\left(\frac{dm_f}{dt} \right)_d = \dot{m}_d = \beta (c_F - c_f) \quad (1)$$

Surface reaction:

$$\left(\frac{dm_f}{dt} \right)_d = \dot{m}_d = k_R (c_f - c_s)^n \quad (2)$$

For a reaction of 2. order it follows:

$$\dot{m}_d = \beta \left\{ \frac{1}{2} \left(\frac{\beta}{k_R} \right) + (c_F - c_s) - \left[\frac{1}{4} \left(\frac{\beta}{k_R} \right)^2 + \left(\frac{\beta}{k_R} \right) (c_F - c_s) \right]^{1/2} \right\} \quad (3)$$

Unsatisfactory is the fact that due to the unknown concentration c_f at the fouling layer surface a detailed look into the deposition procedure is impossible.

More difficult was the lack of knowledge with respect to the solids removal. It depends on the shear stress at the layer surfaces due to the liquid flow, $\tau_f \sim \rho w^2$. For the shear strength of the layer we use an assumption of Bohnet (1987):

$$\sigma_f = k_1 \frac{P}{N x_f (1 + \delta \Delta T) d_p} \quad (4)$$

with P for the intercrystalline force, N number of defects in the fouling layer, x_f layer thickness, σ linear coefficient of thermal expansion, ΔT temperature difference within the fouling layer, d_p crystal size.

For the removal rate can be written:

$$\left(\frac{dm_f}{dt}\right)_r = \dot{m}_r = k_2 \frac{\tau_f}{\sigma_f} \rho_f \left(\frac{\eta g}{\rho}\right)^{1/3} \quad (5)$$

and it follows:

$$\dot{m}_r = k_3 \frac{N}{P} \rho_f (1 + \delta \Delta T) dp (\rho^2 \eta g)^{1/3} x_f w^2 \quad (6)$$

The rate of growth of the layer is:

$$\frac{dm_f}{dt} = \dot{m}_d - \dot{m}_r \quad (7)$$

Introducing the fouling resistance

$$R_f = \frac{x_f}{\lambda_f} \text{ with } x_f = \frac{m_f}{\rho_f} \quad (8)$$

With Eq. (3), (6) and (7) the fouling resistance can be calculated. The only unknown properties are k_3 , N and P . Krause (1986) determined from his experiments with CaSO_4 solutions:

$$\frac{P}{k_3 N} = 83,2 w^{0.54} \quad (9)$$

As example Fig. 2 gives a comparison of measured and calculated fouling resistances. The empirically received Eq. (9) was needed to calculate the shear strength in Eq. (4). It was therefore necessary to have a closer look at the shear strength.

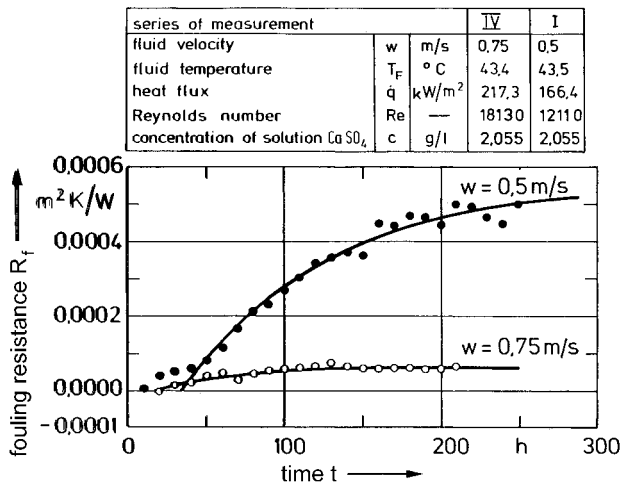


Fig. 2: Fouling curves for a CaSO_4 solution

Shear strength of the fouling layer

To receive information on the shear strength as defined in Eq.(4), Hirsch (1996, 1999) developed a device for the measurement of the shear strength of crystal cylinders. Due to the fact, that the real fouling layers are rather thin he combined the shear strength measurements with a wearing procedure (Fig. 3) and was able to describe the shear strength with the abraded thickness of the fouling layer (Fig. 4).

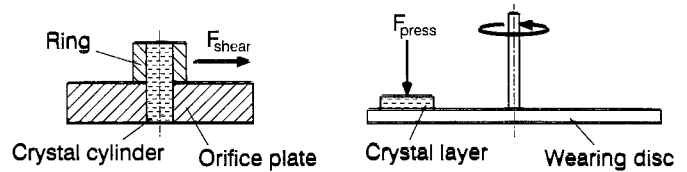


Fig. 3: Shear strength device and wearing disc

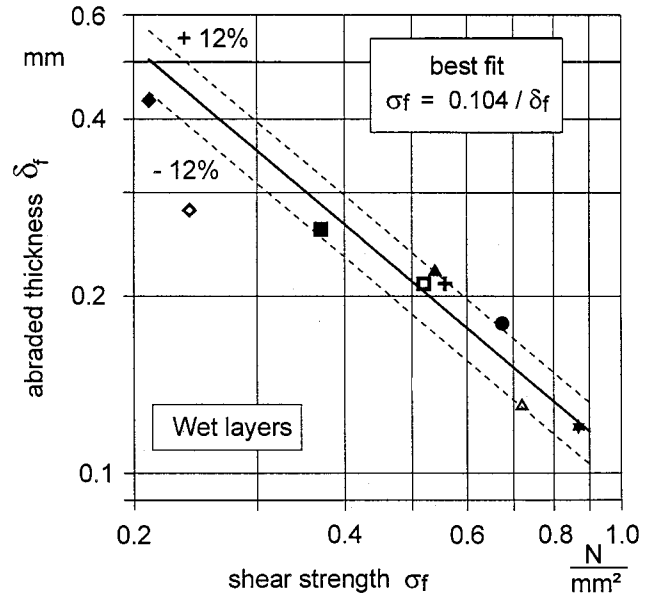


Fig. 4: Abraded fouling layer thickness versus shear strength

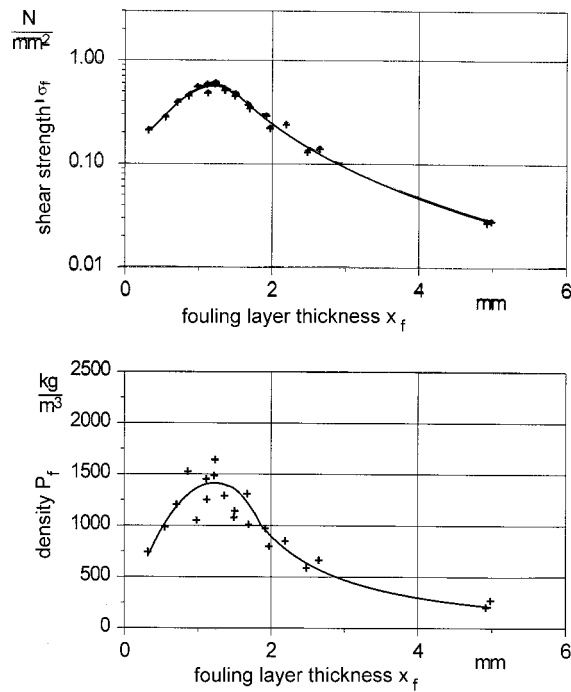


Fig. 5: Shear strength and density versus fouling layer thickness

The shear strength and the density of the fouling layer strongly depend on the layer thickness as shown in Fig. 5. The results were obtained with CaSO_4 layers of a total thickness of about 6 mm. Introducing the shear strength into the model equation gave very good results as shown in Fig. 6.

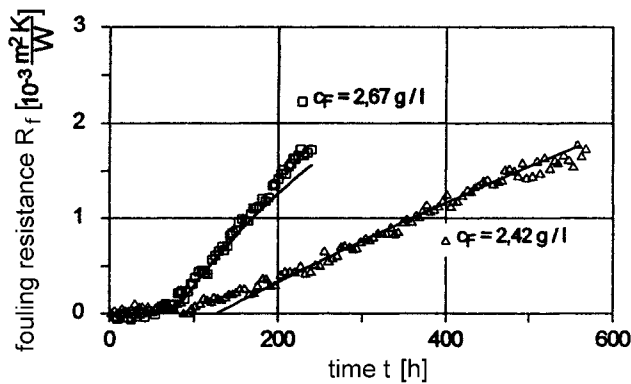


Fig. 6: Measured and calculated fouling resistances for different concentrations

Two wave length holographic interferometry

To receive information on the concentration at the fouling layer surface, Seyfried (1993) measured temperature and

concentration profiles in the vicinity of the surface using two wave length holographic interferometry (Fig. 7). As salt he used Na_2SO_4 . As examples Fig. 8 shows temperature profiles for a clean heat transfer surface and Fig. 9 concentration profiles for progressing crystallization. Drawing the concentration against the temperature an unexpected result was received. In the vicinity of the layer surface a strong supersaturation is observed with a very sharp decline of the concentration directly at the surface as can be seen from Fig. 10.

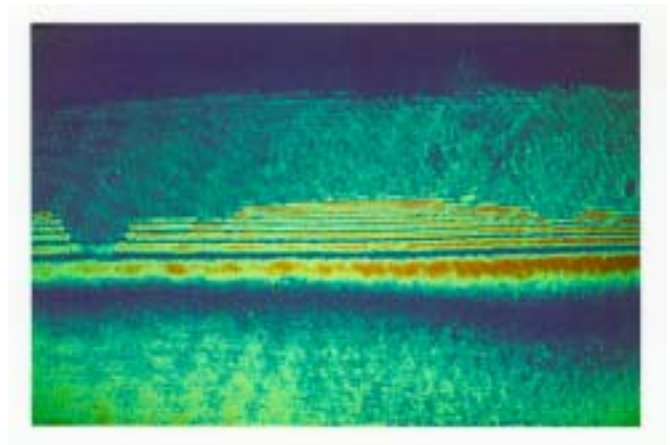


Fig 7: Holographic interferogram with crystallization

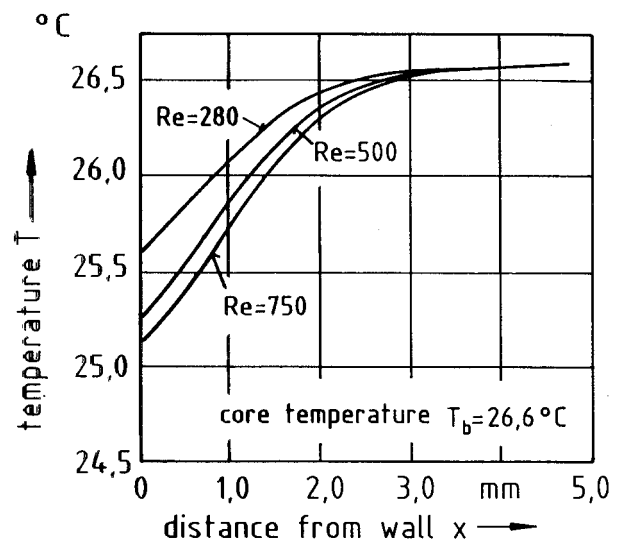


Fig. 8: Temperature profiles without crystallization

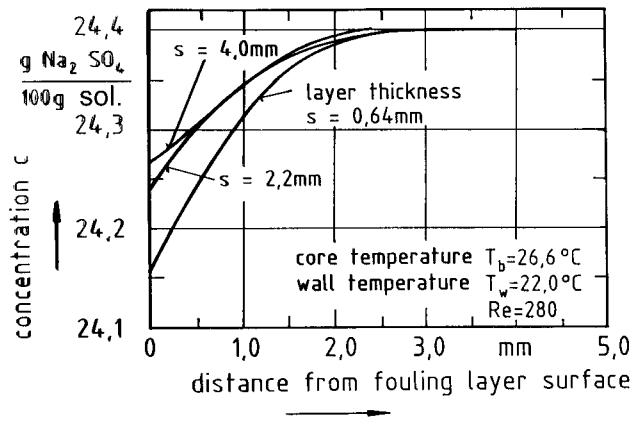


Fig. 9: Concentration profiles for progressing crystallization

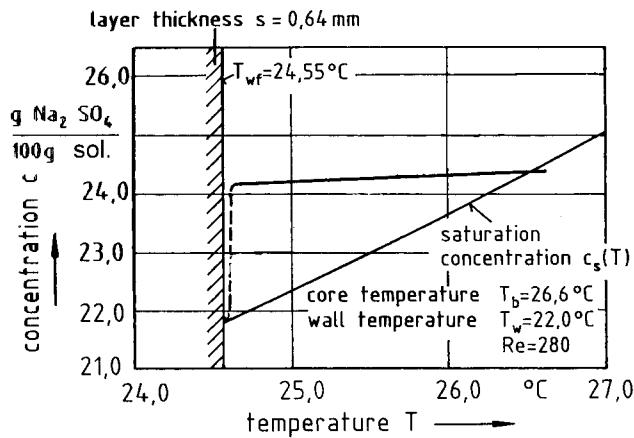


Fig. 10: Concentration versus temperature for a fouling layer of 0,64 mm thickness

Pulsating flow

The question whether a pulsating liquid flow influences fouling was answered by Augustin (2001). Fig. 11 shows the fouling resistance without and with pulsation, Fig. 12 the results in detail. The test runs without pulsation showed the expected decrease of the fouling resistance with increasing flow velocity. Test runs with pulsation led to a little improvement of heat transfer which displays a negative value of the fouling resistance. This is caused by small crystals growing on the heat transfer surface which increase turbulence. Optical observations with a CCD-camera showed that single crystals or small crystal clusters that grew at the surface were removed continuously and started growing at another part of the heat transfer surface. The adhesion force between crystals and surface is lower than the hydrodynamic forces acting on the crystals which means that the crystals can be removed. A quasi-stationary state ensues.

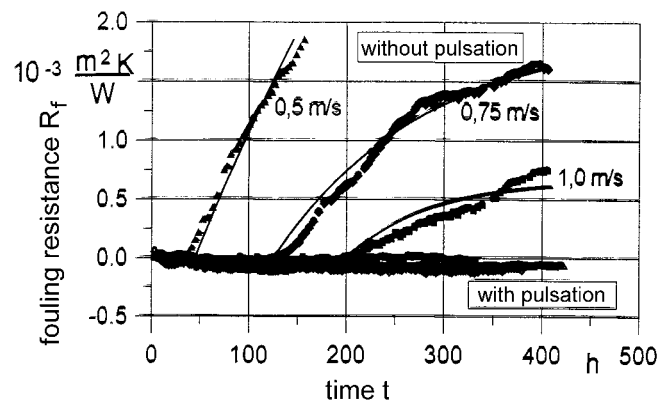


Fig. 11: Fouling curves without and with pulsation of the liquid flow

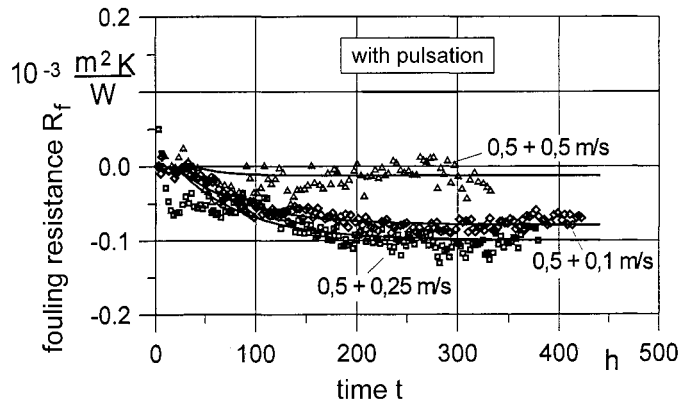


Fig. 12: Fouling curves with pulsation of the liquid flow

Based on these results further investigations were carried out varying the oscillation frequency. Single strokes of higher velocity superimposed on the stationary flow and the time interval were varied. The fouling behaviour of the test runs with short intervals was similar to the experiments with continuous pulsation. Going to longer intervals leads to a limiting value where no difference could be observed between experiments with and without pulsation.

Surface structure

The behavior of structured surfaces is completely different. Augustin (1992, 1993) investigated different structures and received results as shown in Fig. 13. The fouling curves for roughened pipes show a different shape compared to smooth pipes. In the initial region the deposition rate increases, comes to a turning point, decreases and reaches the final value of zero. This initial region can be explained by the fact that during the fouling process the first deposits occur within the roughness of the structure. Once the deposit is sufficient to fill the roughness structure and creates a smooth pipe the fouling curve becomes similar to the curves obtained for smooth pipes. Theoretical calculations of the volume of the deposit required to fill the

roughness structure (dashed lines) show that it is possible to explain the experimental results on this basis.

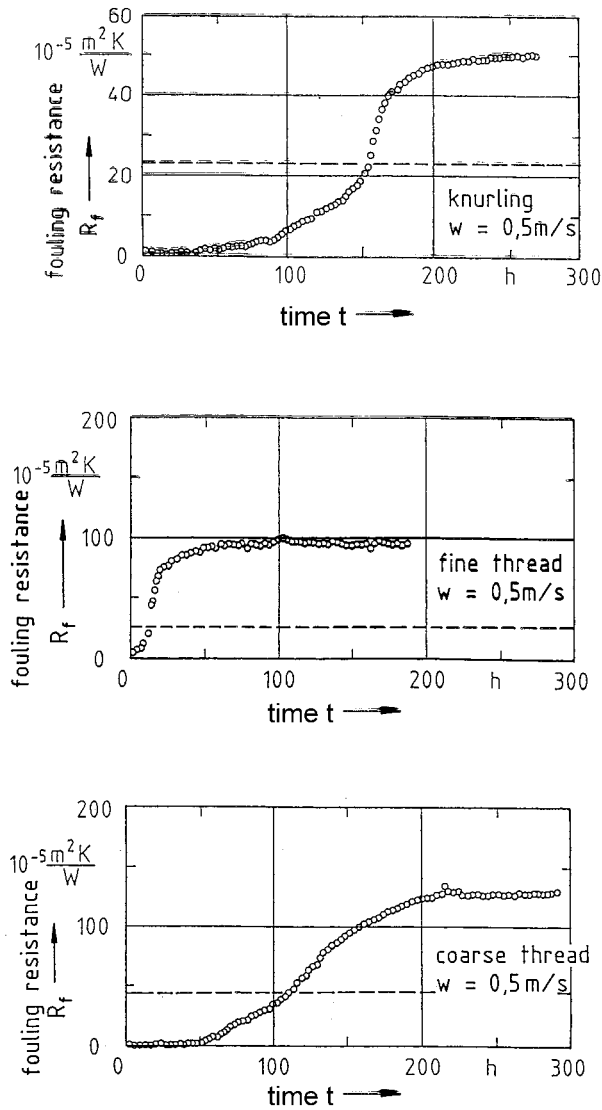


Fig. 13: Fouling resistance depending on time for pipes with knurling and different threads (aqueous solution of $CaSO_4$)

pH-value

A very strong influence shows the pH-value. For $CaCO_3$ solutions Augustin (1992, 1995) determined the asymptotic fouling resistance. The saturation index has been calculated using the reaction equations for the dissociation of $CaCO_3$. From these calculations it can be seen, that the

saturation index is proportional to the deposited mass flow rate of the solids. Experiments have been carried out for the pH-value range of technical interest between pH 6 and pH 10. The results are shown in Fig. 14. The asymptotic fouling resistance increases with the pH-values due to a higher strength of the fouling layer caused by an increasing number of nucleation sides for higher supersaturation. Taking into consideration the complexity of the fouling process the comparison of results of fouling experiments carried out at different pH-values is in good agreement with the calculated data.

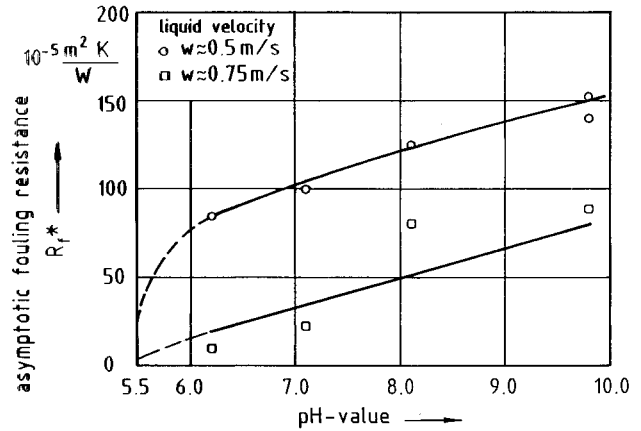


Fig. 14: Asymptotic fouling resistance depending on pH-value and liquid velocity for aqueous solutions of $CaCO_3$ (Temperature 70 – 90 °C)

Modification of the Interface Crystal/Heat Transfer Surface

An approach for fouling mitigation is the reduction of the adhesive strength between the crystals and the heat transfer surface as shown in Fig. 15.

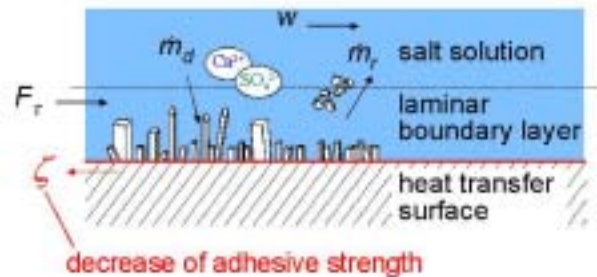


Fig. 15: Approach for fouling mitigation during the induction period

In a first step Förster (1999, 2001) determined the surface free energy by wetting experiments.

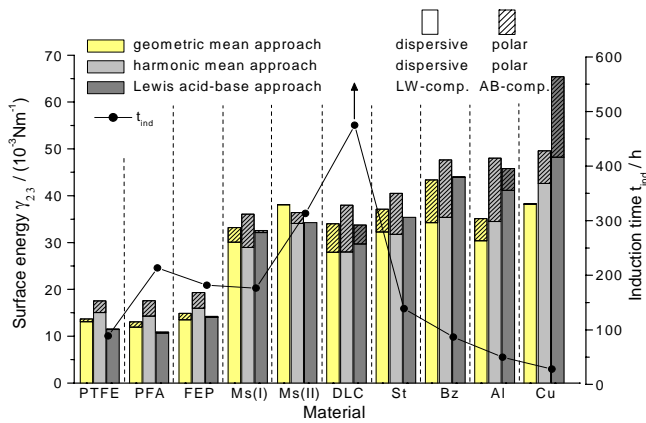


Fig. 16: Surface energy and induction time

A comparison of surface energy and induction time showed, that there is no correlation (Fig. 16). What was really needed was the interfacial energy between crystals and surface, which was determined also by wetting experiments (Fig. 17).

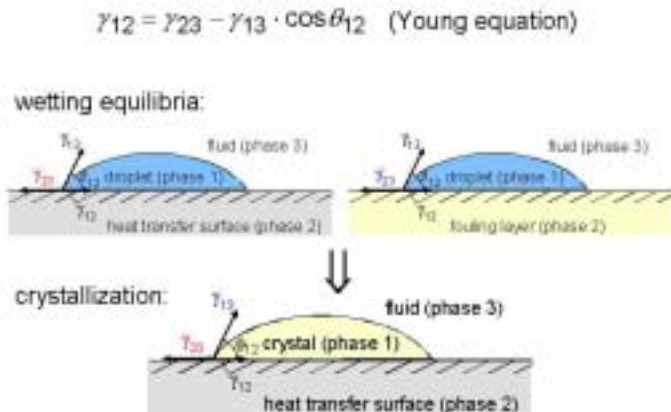


Fig. 17: Interfacial energy crystal/surface

Plotting the induction time against the spreading coefficient (Fig. 18) gave good results for metallic heat transfer surfaces, but could not describe polymeric materials.

spreading coefficient $\lambda_{12} = \gamma_{23} - \gamma_{13} - \gamma_{12}$

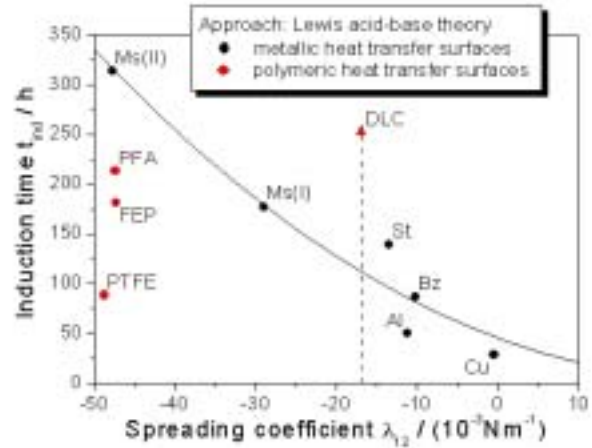


Fig. 18: Interfacial defect model

The reason is, that the roughness of the heated surface has to be taken into account. With the roughness R_z and the width of the elements R_s a surface texture parameter $K = R_z \cdot R_s$ was introduced. Comparing the experimentally received data for a reference topography gave very good results. (Fig. 19)

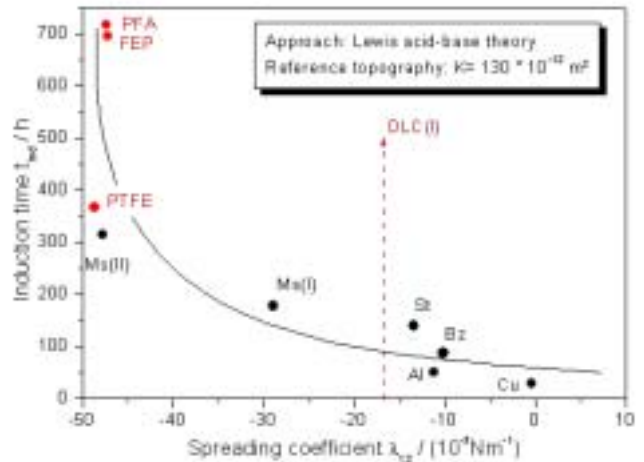


Fig. 19: Induction time versus spreading coefficient

Numerical Simulation

Brahim (2003) simulated the fouling behavior on the basis of a realistic heat flux distribution during the fouling process. His model is shown in Fig. 20, his results in Fig. 21.

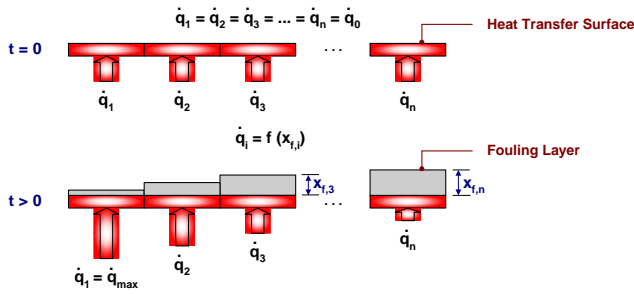


Fig. 20: Realistic distribution of the heat flux along the heat transfer surface.

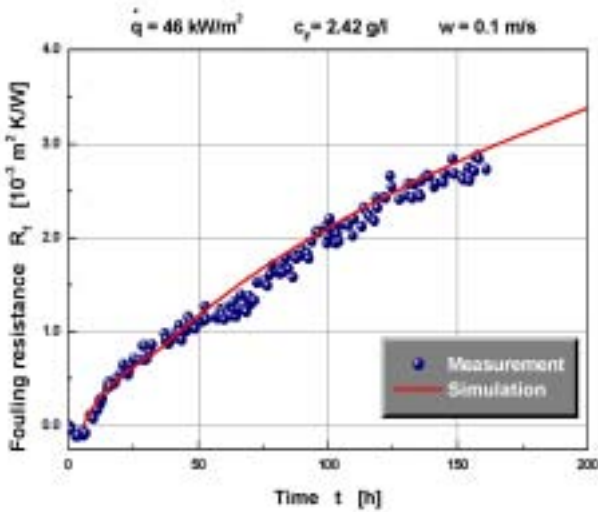


Fig. 21: Comparison of simulation and measurement results

Multi-component systems

The fouling behavior of CaSO₄/CaCO₃ solutions can not be described with the behavior of the single salts. Höfling (2004) determined a strong influence of the pH-value not only on the fouling resistance as shown in Fig. 22 but especially on the structure of the fouling layer which is determined by different modifications of the crystals (Fig. 23).

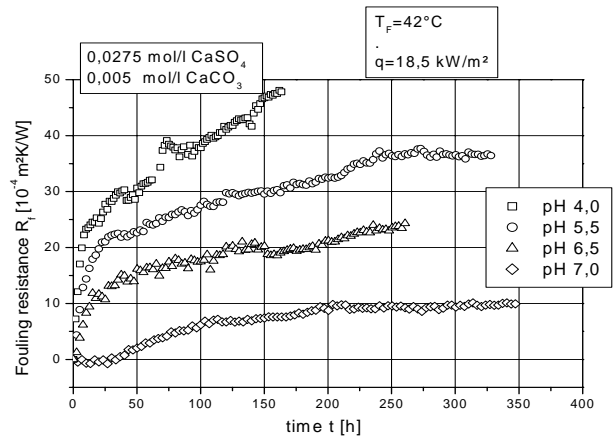


Fig. 22: Fouling resistance for different pH-values



Fig. 23: Heating element

CONCLUSIONS

This paper summarizes the results of fouling research at the Technical University of Braunschweig. The author thanks with great respect his PhD.-students working in this field. They performed their research with great enthusiasm and ability. It was a real pleasure having them at the institute.

NOMENCLATURE

c_F	concentration of salt solution	[kg/m ³]
c_S	saturation concentration	[kg/m ³]
c_f	concentration in the vicinity of the fouling layer	[kg/m ³]
D	diffusion coefficient	[m ² /s]
g	gravitational acceleration	[m/s ²]
P/k_3	cohesion coefficient	[kg m/s ²]
k_R	rate of reaction	[m ⁴ kg/s]
\dot{m}	total mass rate	[kg/m ² s]
\dot{m}_d	deposition mass rate	[kg/m ² s]
\dot{m}_r	removal mass rate	[kg/m ² s]
n	order of the surface reaction	[-]
P	intercrystalline adhesion force	[N]
\dot{q}	heat flux	[W/m ² K]
R_f	fouling resistance	[W/m ² K]
T_f	temperature of fouling layer surface	[K]
T_F	temperature of salt solution	[K]
x_f	thickness of crystal layer	[m]
w	fluid velocity	[m/s]
t	time	[s]
T	temperature	[K]
β	mass transfer coefficient	[m/s]
γ_i	surface energy	[N/m]
η	viscosity of salt solution	[kg/m s]
λ_f	thermal conductivity of the fouling layer	[W/m K]
$\lambda_{1,2}$	spreading coefficient	[N/m]
θ	contact angle	[°]
ρ	density of salt solution	[kg/m ³]
ρ_f	density of fouling layer	[kg/m ³]
σ_f	shear strength	[N/m ²]
τ_f	shear stress	[N/m ²]
ζ	adhesive strength	[N/m ²]

REFERENCES

- W. Augustin, 1992, Verkrustung (Fouling von Wärmeübertragungsflächen, *Diss. TU Braunschweig*)
- W. Augustin, M. Bohnet, 1995, The influence of the ratio of free hydrogen ions on crystallisation fouling, in *Chem. Eng. Process.* 34, 2, p. 79-85
- W. Augustin and M. Bohnet, 2001, Influence of pulsating flow on fouling behaviour, in: *Mitigation of heat exchanger fouling and its economic and environmental implications*, eds. T.R. Bott et al., Begell House, New York, pp. 161-168
- M. Bohnet, 1987, Fouling of heat transfer surfaces *Chem. Eng. Techn.* 10, 2, p. 113-125
- M. Bohnet, W. Augustin, 1993, Effect of surface structure and pH-value on fouling behaviour of heat exchangers in: *Transport Phenomena in Thermal Engineering*, eds. J.S. Lee et al., Begell House, New York, p. 884-889
- F. Brahim, 2003, Numerische Simulation des Kristallwachstums auf wärmeübertragenden Flächen (Fouling), *Diss. TU Braunschweig*
- F. Brahim, W. Augustin, M. Bohnet, 2003, Numerical simulation of the fouling process, *Int. J. of Therm. Sci.* 42, 3, p. 323-334
- M. Förster, M. Bohnet, 1999, Influence of the Interfacial Free Energy Crystal/Heat Transfer Surface on the Induction period during Fouling, *Int. J. Th. Sci.* 38, p. 944-954
- M. Förster, 2001, Verminderung des Kristallisationsfouling durch gezielte Beeinflussung der Grenzfläche zwischen Kristallen und Wärmeübertragungsfläche, *Diss. TU Braunschweig*
- H. Hirsch, 1996, Scher- und Haftfestigkeit kristalliner Foulingsschichten auf wärmeübertragenden Flächen, *Diss. TU Braunschweig*
- H. Hirsch, W. Augustin, M. Bohnet, 1999, Influence of fouling layer shear strength on removal behaviour, in: *Understanding Heat Exchanger Fouling and its Mitigation*, eds. T.R. Bott et al., Begell House, New York, p. 201-208
- V. Höfling, 2004, Kristallisationsfouling auf wärmeübertragenden Flächen durch Mehrkomponentensysteme, *Diss. TU Braunschweig*
- V. Höfling, W. Augustin, M. Bohnet, 2004, Crystallization fouling of the aqueous two-component system CaSO₄/CaCO₃ – Fouling of salt mixtures, *Int. J. Trans. Phenomena* 6, 2, p. 99-109
- S. Krause, 1986 and Translation 1993, Fouling an Wärmeübertragungsflächen durch Kristallisation und Sedi- mentbildung, *Diss. TU Braunschweig*, Fouling of heat-transfer surfaces by crystallization and sedimentation, in *Int. Chem. Eng.* 33, 3, p. 355-401
- F. Seyfried, 1993, Untersuchung der Kristallisation von Salzen an wärmeübertragenden Wänden mit Hilfe der holographischen Interferometrie, *Diss. TU Braunschweig*